Development of a hybrid cutting force model for micromilling of brass

Huaizhong Li[1, 2] *, Bing Wu[2]

[1] Griffith School of Engineering, Gold Coast campus, Griffith University, QLD 4222, Australia

[2] School of Mechanical and Manufacturing Engineering, The University of New South Wales, Sydney, NSW 2052, Australia

*** Corresponding Author**: Dr Huaizhong Li, Griffith School of Engineering, Gold Coast campus, Griffith University, QLD 4222, Australia.

E-mail: lihuaizhong@gmail.com; h.li@griffith.edu.au.

Telephone: +61 (7) 5552 8252; Facsimile: +61 (7) 5552 8062

Abstract: Modelling of the cutting forces in micromilling is challenging due to the size effect and existence of a minimum chip thickness. This paper presents the development of a cutting force model for micromilling of brass. The prediction of cutting forces derives from a simplified orthogonal process. A finite element (FE) model is employed to simulate two-dimensional cutting forces in orthogonal micro cutting, with the ploughing and tool edge effect taken into consideration. The flow stress of workpiece material is modelled by using the Johnson-Cook constitutive material law. The FE model is used to evaluate the critical chip thickness and to extract the cutting force coefficients. The cutting force coefficients are modelled as a function of instantaneous uncut chip thickness, which is independent of cutting speed but influenced by tool edge radius. To rectify the issue of sharp increase of the force coefficients under very small uncut chip thickness, a critical uncut chip thickness

value is introduced and the coefficients are adjusted by using a tangent slope for uncut chip thickness smaller than the critical value. A generalized analytical force model based on numerical findings is developed to predict the micro milling force by considering the tool trajectory and tool runout. The simulation results of micro milling forces are compared against experimental measurement, where an agreement of force trends is shown along with the increasing feedrate and depth of cut.

Keywords: Micromilling; Cutting forces; Model; Brass; Finite element method; Machining.

1. Introduction

Recent advances in miniaturization have led to the understanding and development of small scale components that require advanced machining techniques in order to achieve the tolerances and feature sizes required. Micromilling is one of the most efficient manufacturing methods for micro feature fabrication in biomedical, optics and electronics industries. The mechanical modelling of micro milling process has been a research topic attracting many researchers to explore the mechanics and to investigate the influences of the machining parameters for improved productivity and quality [1,2].

Modelling of the cutting forces in micromilling is challenging due to the size effect (also known as the edge radius effect) and existence of a minimum chip thickness [3,4]. Extending conventional mechanical machining into the micro-scale may seem obvious, but this has not been straightforward as the physics and engineering involved in the down-scaling has brought about new challenges [4]. In comparison to macro-

milling, the dimensions of chip loads and tool geometry for micro-milling operations are typically an order of lower magnitude. The workpiece does not see a sharp cutting edge. This results in the cutting edge rubbing or ploughing the workpiece rather than cutting. Ploughing or rubbing causes a significant increase of cutting force as the frictional forces are increased, which can also lead to the onset of vibrations and reduced surface quality [5–7]. The ploughing is often referred to as the size effect in micromachining. There is a substantial increase in the specific energy required with a decrease in chip size during machining.

In micromachining, formation of the chip is influenced by the minimum chip thickness to successfully remove the workpiece layer as a single chip. When attempting to cut less than the minimum chip thickness, the workpiece material preferentially compresses and springs back after the passage of the cutting edge. If the cutting edge attempts to take exactly the minimum chip thickness, a chip less than the minimum chip thickness is formed as part of the surface is compressed during cutting and this springs back up after the cutting edge has passed. A fully formed chip is produced only when a chip larger than the minimum chip thickness is removed in a single cut [8]. Vogler et al. [6,7] incorporated the effect of minimum chip thickness by modelling the deformation forces as being proportional to the volume of the interface between the tool and workpiece base using an interference mechanism. They showed that the minimum chip thickness causes the cutting forces and surface roughness to increase at low feed-rates. Yuan et al. [9] formulated an expression relating the minimum chip thickness to the cutting edge radius and friction coefficient whereby the minimum chip thickness increases linearly with the cutting edge radius.

In a mechanistic model the force required to remove a chip is related to the chip thickness, the width of the cut and the material coefficient. The material coefficient is usually obtained from experimental force measurements. As the forces are three dimensional in nature, the distribution of the forces is often assumed to be distributed in a fixed ratio. Bao and Tansel [10] developed a cutting force model of micro-end-milling based on the conventional model by Tlusty and Macneil [11]. Zaman et al. [12] proposed a three-dimensional force model as a new concept to improve the cutting force estimation in micro-end-milling by calculating theoretical chip area instead of the undeformed chip thickness. However, errors can occur due to the consideration of only projected area. Kang et al. [13] presented an analytical mechanistic model of micro end milling for predicting the cutting force, which considered the tool–workpiece contact at the flank face. Park and Malekian [14] studied the mechanistic modeling of shearing and ploughing domain cutting regimes, and used the Kalman filter compensation method to measure the forces to obtain the cutting constants. Srinivasa and Shunmugam [15] presented a methodology for predicting the cutting coefficients considering the edge radius and material strengthening effects for a mechanistic force model of micro end milling.

However, in the mechanistic cutting force models, there is a need for the cutting force coefficients to be determined mainly through experimental extraction. The resultant parameters using this method are highly dependent on specific tool-workpiece pair, which means that the magnitude of cutting force may not be the same as prediction when undertaking the cutting experiment by different tool geometry [2]. It is both costly and time-consuming to conduct the cutting experiments to determine the cutting force coefficients. For new combinations of tools and materials without testing

data, the cutting forces cannot be predicted using this approach. The finite element method (FEM) has been well established and widely used to model the chip formation process. For the micromilling operation, the cutting forces can be obtained directly from FEM simulation theoretically. Liu and Melkote [16] employed a strain gradient plasticity based finite element model for orthogonal micro-cutting to predict the cutting forces and specific cutting energy in micro-cutting of an aluminum alloy in order to investigate the role of the tool edge radius on size effect. Jin and Altintas [17] predicted micro-milling forces with finite element method for Brass 260. The cutting force coefficients were evaluated from a series of finite element simulations. The algorithms were integrated into an existing milling process simulation system to predict micro-milling forces, vibrations, dynamic chip thickness and surface form errors. Their results showed that the micro-milling forces in the feed direction were estimated less accurately. It should be noted that although three dimensional (3D) analysis of micro cutting offers more realistic simulation of the process, most of the current simulation models using FEM for the prediction of fundamental variables and machining performance measures are two dimensional (2D), which are based on the hypothesis of orthogonal cutting [18]. This is possibly due to the advantages of computational efficiency, simplicity, stability, and mature techniques associated with the 2D approaches [2].

Brass is material widely used for micro parts in the electronics and telecommunication field due to its properties such as good electrical and thermal conductivity and malleability [19]. This paper presents the development of a new cutting force model for micromilling of brass. The prediction of cutting forces derives from a simplified orthogonal process. A finite element (FE) model is employed to simulate two-

dimensional cutting forces in orthogonal micro cutting for the determination of the cutting force coefficients. The flow stress of workpiece material is modelled by using the Johnson-Cook constitutive material law. A comparison of the simulation and experimental results is also introduced.

2. Model development

Modelling of cutting force in milling operation is usually carried out by geometric and kinematic transformation of cutting force components based on an orthogonal cutting process. A two-dimensional (2D) finite element (FE) model of orthogonal micro-cutting considering tool geometry and material properties is firstly developed in this study by using LS-Dyna as the platform. A schematic of the FE model is shown in Figure 1, with the workpiece and cutting tool geometries included. The key geometric parameters and cutting conditions are listed in Table 1. As steady state conditions are assumed, the width of cut is derived by plane strain element deformation, which is considered in the 2D modelling. The displacement and rotation of the nodes on the bottom and one side of the workpiece are fixed. In the 2D FE model, the tool is modelled as rigid body, the heat transfer between tool and workpiece is neglected, the velocity of tool's motion is assumed as constant, and plain strain assumption for 2D elements is applied.

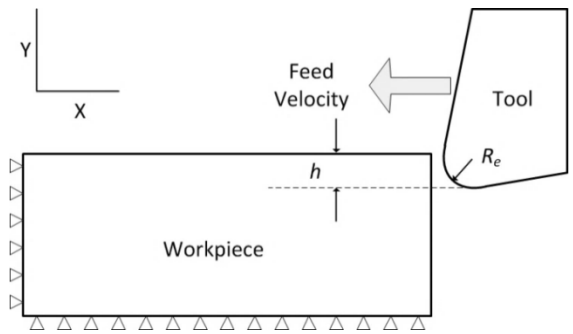

Figure 1. Schematic of a 2D finite element model of orthogonal cutting

As shown in Figure 1, the cutting direction of the tool is towards the horizontal arrow mark. A global boundary plane is applied to the left and bottom side of the workpiece. Adaptive meshing method is used. Friction occurs at the contact area between the tool surface and workpiece. Coulomb friction is used to model the friction stress at the tool-workpiece contact. The friction coefficient is assumed to be dependent on the relative velocity v_{rel} of the surfaces in contact.

Table 1 Geometry and cutting conditions in FE model

Tool Rake angle	6°
Tool Clearance angle	12°
Tool edge radius (R_e)	4 μm
Width of cut	0.05 mm
Length of cut	0.16 mm
Workpiece dimensions	0.2 mm × 0.04mm
Uncut chip thickness	0.2 μm to 10 μm
Cutting speed	320 mm/s to 750 mm/s (approximately 19 m/min to 45 m/min)

Table 2 Johnson-Cook parameters for the material model [20]

Material	A[MPa]	B[MPa]	C	n	m	Melt Temp. [K]
Brass	112	505	0.009	0.420	1.68	1189

One important step in metal cutting simulation is modelling flow stress of workpiece material. Flow stress is an instantaneous stress that results in the material flow and it depends on strain, strain rate and temperature. The flow stress can be represented by mathematical forms of constitutive equation. The Johnson-Cook constitutive material model [20] is used to model the workpiece flow stress behaviour. Although it has been argued that the material can be of the same order as the grain size and cannot be treated as isotropic and homogeneous in micro machining modeling [21], the

Johnson–Cook model has been widely accepted in machining simulation and micromachining simulation, due to its good fit for strain-hardening and thermal softening behavior of metals and its numerical robustness, and it can be easily used in finite element simulation models [22,23]. The model presented by Johnson and Cook expresses the flow stress as a factor of strain, strain rate and temperature effects, and the universal equation is given by:

$$\sigma = \left[A + B\left(\epsilon_{\mathrm{p}}\right)^{\mathrm{n}}\right]\left[1 + C\, ln\left(\frac{\dot{\epsilon_{\mathrm{p}}}}{\dot{\epsilon_0}}\right)\right]\left[1 - \left(\frac{T - T_{room}}{T_{melt} - T_{room}}\right)^{\mathrm{m}}\right] \qquad (1)$$

where the *A*, *B*, *n*, *C*, *m* are the five constants for specific material; ϵ_{p} is the equivalent plastic strain, $\frac{\dot{\epsilon_{\mathrm{p}}}}{\dot{\epsilon_0}}$ is the dimensionless plastic strain rate, T_{room} is the room temperature, T_{melt} is melting temperature, and the expression $\frac{T-T_{room}}{T_{melt}-T_{room}}$ gives the homologous temperature of the material.

Under the condition without heat-transfer as one of the assumptions, the temperature change in the simulation is computed by the total internal energy including the plastic strain influence for Johnson-Cook material model. The Johnson-Cook parameters for brass used in this study are listed in Table 2.

The mesh design in the 2D FE model is shown in Figure 2. Lagrangian adaptive meshing is applied to account for the severe distortion in the elements of the workpiece as metal machining is a highly deformable process with large plastic strains occurring. This approach helps to avoid excessive distortions of the elements around the tool edge. On the other hand, since the cutting tool is regarded as rigid body, the tool tip and part of the rake face are modelled with higher meshing density

to obtain more accurate results. The elements of workpiece are remeshed continually during the simulation process. A balance between the adaptive frequency and adaptive size in the simulation needs to be found in order to obtain better deformation quality and simulation time. By optimising the process parameters, it has been found that the most efficient simulation process can be realised by setting time interval of 2 μs and adaptive size of 0.9 μm. These results are then used to conduct a series of simulations to predict the cutting forces under different conditions.

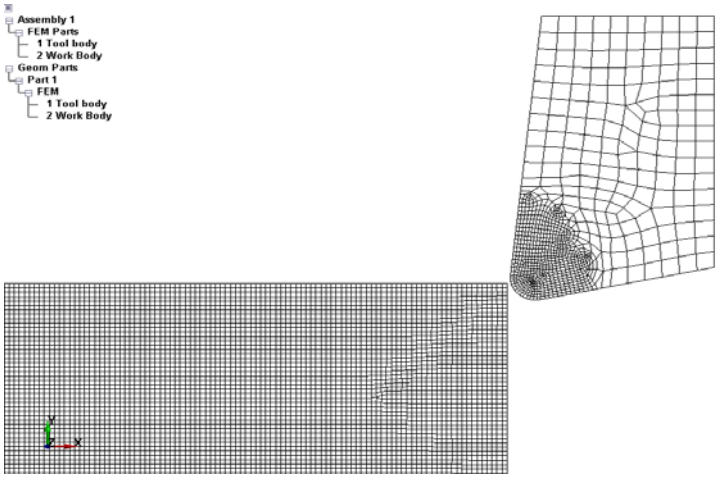

Figure 2. Mesh design in 2D FE model

To assess the stress and strain distribution at the deformed zone, the steady state simulation results under the conditions of 4 μm uncut chip thickness and 28 m/min cutting velocity have been used for a case study. It shows that high Von-Mises stresses around 650 MPa are distributed at primary shear zone, and also at the secondary shear zone where the chip and the rake face of the tool are mainly in contact, as shown in Figure 3(a). High plastic strain extends along the secondary shear zone with a maximum value of 3.1, and it mostly remains at the contact area around the tool tip, as shown in Figure 3(b).

To investigate the relationship between minimum chip thickness and tool edge radius, several simulations of micro orthogonal cutting are conducted with uncut chip thickness *h* varying from 0.2 μm to 2 μm, as shown in Figure 4. When *h* is 0.2 and 0.4 μm (Figure 4(a) and (b)), there is no chip formed. The uncut chip thickness is below a critical value, thus the ploughing effect without chip formation is dominant. Chip formation becomes observable when *h* is 1 μm, and it turns out with forming chip when *h* is higher than 1.5 μm (Figure 4(e) and (f)). The chip formation is mainly contributed by shearing behaviour when uncut chip thickness is higher than the critical value. It seems difficult to determine a certain value from the simulation as the minimum chip thickness below which no chip forms. However, a critical chip thickness can be approximately determined at a ratio between 0.2 and 0.5 of the tool edge radius.

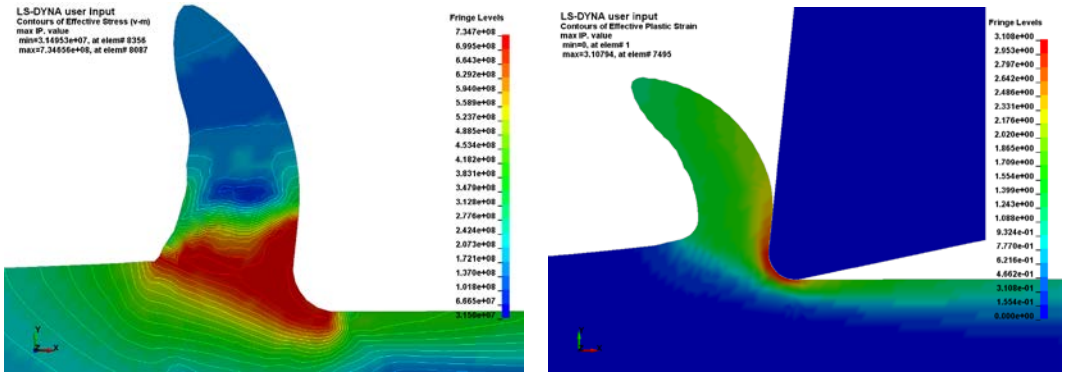

(a) (b)

Figure 3. Predicted (a) Von-Mises stress variations, (b) effective plastic strain, at steady state in the simulation with: uncut chip thickness 4 μm, cutting velocity 28 m/min.

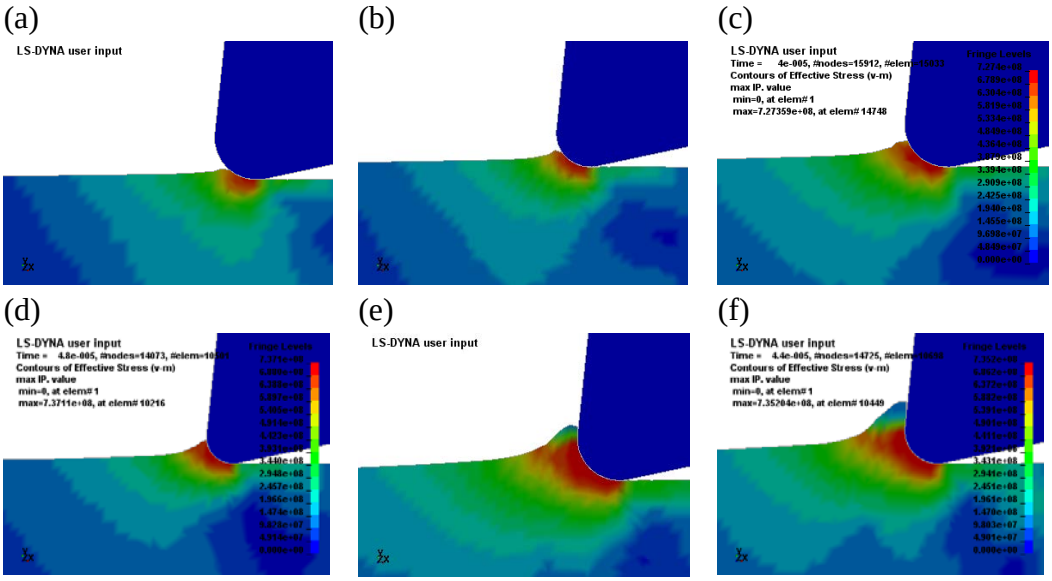

Figure 4 FE simulations of micro orthogonal cutting, with the Von-Mises stress distribution shown in different colours. Tool edge radius R_e = 4 μm. Uncut chip thickness: (a) 0.2 μm (=0.05R_e), (b) 0.4 μm (=0.1R_e), (c) 0.5 μm (=0.125R_e), (d) 0.6 μm (=0.15R_e), (e) 1 μm (=0.25R_e), (f) 1.5 μm (=0.375R_e).

A series of simulation studies are carried out on cutting brass at different uncut chip thickness and cutting speed. The cutting force outputs are recorded as force rate component, which is a ratio between cutting force (N) and width of cut (mm), in 2D simulations. The cutting force rate variation vs. cutting speed under a fixed uncut chip thickness of 5 μm is shown in Figure 5 (a). When the cutting speed increases from 19 m/min to 45 m/min, there is only slight force variation of less than 5%. It can be concluded that both tangential and normal forces are not sensitive to the change of cutting speed in this range. Figure 5(b) illustrates the cutting force rate results at different uncut chip thickness. The tangential force rate increases from 3.5 N/mm to 18 N/mm when the uncut chip thickness increases from 0.2 μm to 10 μm. However,

there exists a slight decrease of the normal force rate along with the increase of the uncut chip thickness.

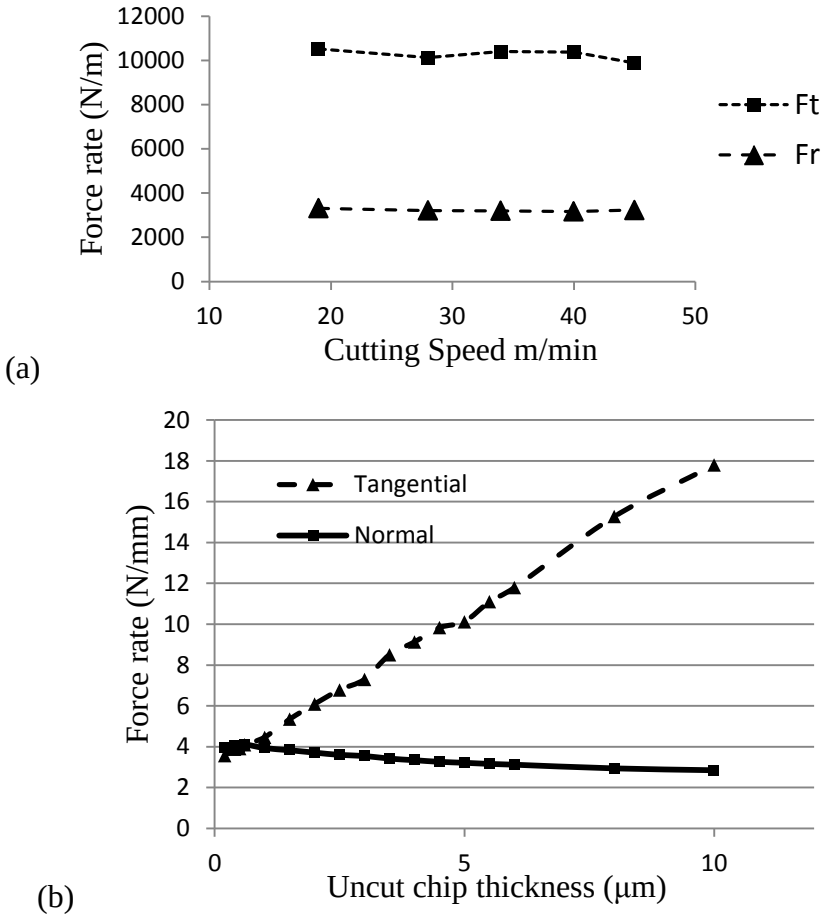

Figure 5. Cutting force variation vs. (a) cutting speed, with fixed uncut chip thickness 5 μm; (b) uncut chip thickness. Tool edge radius: 4 μm.

To develop a cutting force model in micro milling, a few assumptions are made for simplification. Only the cutting forces in the plane perpendicular to the tool axis are considered. At a given time instant, the cutting deformation in the micro milling is approximated as orthogonal machining process. The instantaneous uncut chip thickness in milling process is regarded as equivalent to that in an orthogonal cutting. The cutting force coefficients are determined from numerical simulation results by the

FE model as introduced, which can account for ploughing effect in micro machining. These coefficients are express as a nonlinear function of the instantaneous uncut chip thickness. A relationship between the cutting forces and the chip load can be modelled by using the coefficients (K_t, K_n) as

$$\begin{cases} F_t = K_t(h)hw \\ F_n = K_n(h)hw \end{cases} \quad (2)$$

where F_t and F_n are the tangential and normal force components, h is the uncut chip thickness, w is the width of cut.

The force rate components (F_t/w) and (F_n/w) are obtained from 2D simulation of micro orthogonal cutting as given in Figure 5(b). They represent the tangential and normal forces on the horizontal plane in milling operation. Then the coefficients K_t and K_n can be found as the force rate components divided by the corresponding uncut chip thickness h. Under a specific cutting condition, the resultant cutting force coefficients as a function of the uncut chip thickness (h) can be determined by non-linear curve fitting of the simulated force rates as follows:

$$\begin{cases} K_t(h) = \alpha_t \cdot h^{p_t} + \beta_t \cdot h^{q_t} \\ K_n(h) = \alpha_n \cdot h^{p_n} + \beta_n \cdot h^{q_n} \end{cases} \quad (3)$$

A set of the parameters (α, β, p and q) estimated through the curve fitting process are listed in Table 3. It should be noted that the ploughing effect is included in the determination of the force coefficients K_t and K_n because the simulated cutting force variation curve vs. uncut chip thickness covers the range in which the edge radius effect is fully accounted. The coefficients are actually functions of the uncut chip thickness, which count in the power law relation between the ploughing effect and the

uncut chip thickness. Since the cutting speed within the simulation range has limited effect on the cutting forces, the coefficients are treated as independent of the cutting speed in the present model.

Table 3 Estimated constants for the cutting force coefficients of brass

	α	β	p	q
K_t [N/mm^2]	252.9	-0.3833	0.08159	-1.39
K_n [N/mm^2]	1.597	-1.16	-0.01627	-1.581

Due to the edge radius effect, there is a substantial increase in the specific energy required with a decrease of chip size during machining. This could be caused by the fact that all metals contain stress reducing defects such as grain boundaries, missing atoms and impurities. When the size of the material to be removed is decreased, the probability of encountering one or more defect decreases leading to the increase in specific energy required for machining. However, an issue of Equation (3) for the coefficients modelling is that the resultant coefficients increase sharply in the region of very small uncut chip thickness and it cannot be directly applied to the prediction of the micro milling force components. It may lead to overestimation of cutting forces at very low uncut chip thickness. A rectification of the coefficients is needed by introducing a critical uncut chip thickness (h_t), which is expressed as

$$h_t = \eta R_e \tag{4}$$

where R_e is the tool edge radius, η is a factor used to determine the critical chip thickness value and it can be determined from numerical simulation results. The

critical uncut chip thickness is used to divide the original coefficients output into two regions. When the uncut chip thickness is equal to or greater than this critical value ($h \geq h_t$), the coefficients remain the same as identified by using Equation (3). When h is less than h_t, the coefficients are adjusted according to Equation (5) by using a tangent slope at the point of h_t.

$$\begin{cases} K_t(h) = \Delta_t h + K_{tm} - \Delta_t h_t \\ K_n(h) = \Delta_n h + K_{nm} - \Delta_n h_t \end{cases} \quad \text{when } h < h_t \qquad (5)$$

where K_{tm} and K_{nm} are the coefficients of K_t and K_n at the critical uncut chip thickness h_t, Δ_t and Δ_n are the estimated slopes of K_t and K_n at the vicinity of h_t. The results of the adjusted cutting force coefficients are shown in Figure 6. In this estimation, η is set as 0.4 based on the numerical simulation results of the critical chip thickness. The fitted results cover the coefficients at two regions which are computed form Equations (2-5).

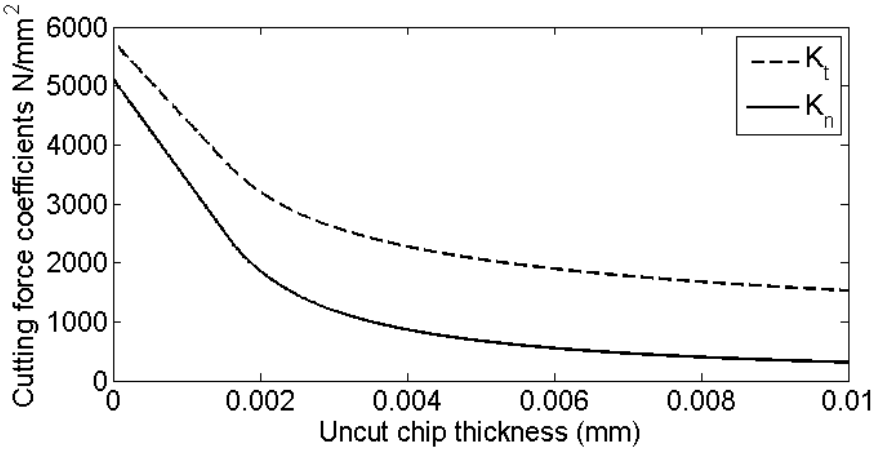

Figure 6. Results of the cutting force coefficients with respect to the uncut chip thickness.

In the micromilling operation, the teeth of the milling cutter enter and exit the work during each revolution. Due to the feature of interrupted cutting action, the undeformed chip thickness varies periodically as the tool rotates. To determine the instantaneous uncut chip thickness for cutting force prediction, a common approach is to assume a circular tool path, which has been used in many existing models. It is to express the chip thickness h as a function of time dependent tool's angular position and feed per tooth:

$$h(\phi) = f_t \sin(\phi) \tag{6}$$

This approximation neglects the cyclical effect on the actual tool path. Although it simplifies the analysis in traditional milling model, it cannot satisfy the precision requirement in micro milling. In the present model, the instantaneous chip thickness is evaluated using a method presented in [24] which is based on the true tooth trajectory. The equation is given by

$$h(\phi) = r\left(1 - \left(1 - \frac{2f_t \sin\phi}{r + (N_t f_t/2\pi)\cos\phi} - \frac{f_t^2 \cos 2\phi}{(r + (N_t f_t/2\pi)\cos\cos\phi)^2} + \frac{f_t^3 \sin\phi \cos^2\phi}{(r + (N_t f_t/2\pi)\cos\phi)^3}\right)^{1/2}\right) \tag{7}$$

where ϕ is the instantaneous angular position of the tooth edge, N_t number of teeth, f_t feed per tooth, and r tool radius.

To account for the helix angle of a micro end mill cutter, the cutter can be discretised into L_a number of slices along its axial direction, using a similar approach as detailed in [25]. Since the main concern is the cutting forces in the *xy* plane which is normal to the cutter axis, at each slice, the cutting action of an individual tooth segment can be

approximated as orthogonal cutting. The angular distance of the cutting edge segment for a tooth at the next slice element is determined by considering the helix angle and the slice thickness. The instantaneous angular position of a tooth edge segment is used to calculate the uncut chip thickness and instantaneous cutting force coefficients. Then the tangential and normal (or radial) force components, i.e., F_t and F_n , acting on any cutting edge segment with a differential axial depth of cut d_a , are determined as

$$\begin{cases} dF_t = K_t h(\phi) d_a \\ dF_n = K_n h(\phi) d_a \end{cases} \tag{8}$$

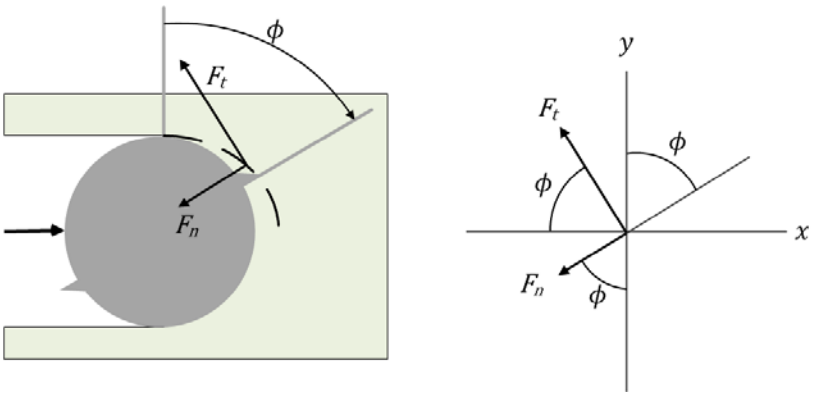

Figure 7 Coordinate system in the model, x is the feed direction and y is normal to feed direction

In this study, the effect of cutter runout is modelled by considering the effective feed which is influenced by each individual tooth and the previous tooth. It means that a modification is needed for the resultant uncut chip thickness. The resultant tangential and normal force components can be projected to the x and y directions as shown in Figure 7 based on the instantaneous rotation angle ϕ by

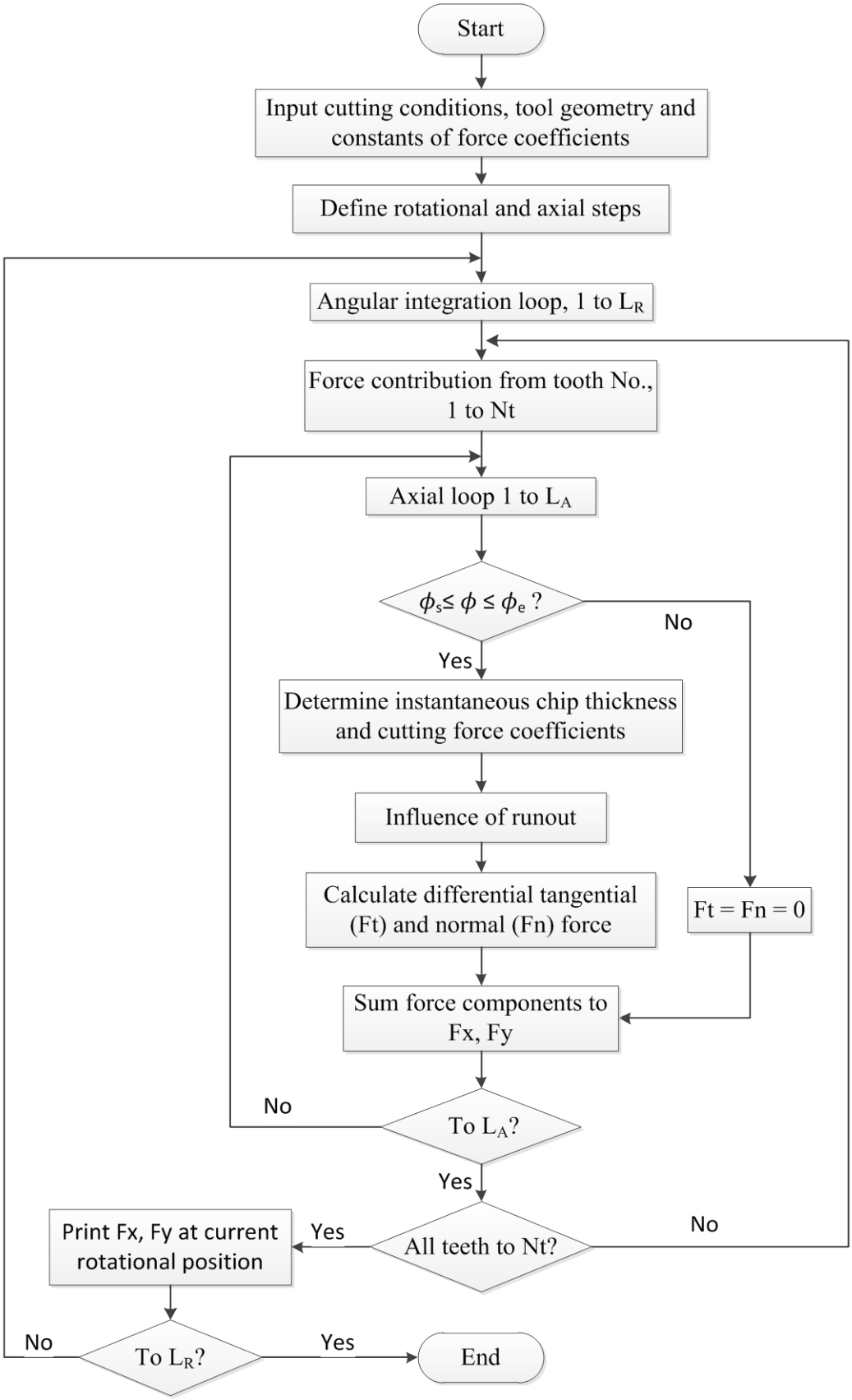

Figure 8. The flowchart of the computation process for the proposed force model

$$\begin{cases} F_x = -F_t \cos\phi - F_n \sin\phi \\ F_y = F_t \sin\phi - F_n \cos\phi \end{cases} \quad (9)$$

In the *xy* coordinate, x is the feed direction and y is normal to feed. The elemental force components evaluated by Equations (6-9) are solved by discretising the axial depth of cut into small axial segments and also incorporating with multiple teeth of the tool. The effect of tool helix on angular position at each axial step is also taken into account. The flowchart of the computation process for calculating micro milling forces using the proposed model is presented in Figure 8.

3. Experimental verification

A Deckel-Maho DMU-P60 precision 5-axis CNC machining centre was used in the cutting experiments. The cutting tools used in micro milling experiments were carbide flat end mills with a diameter 0.9 mm. The tools have two flutes and a helix angle of approximately 30 deg. The workpiece was designed with a base and a rectangular block of length 60 mm and width 8 mm on the top. The base acted as a fixture connected on the dynamometer surface by screws. The material removal was carried out by feeding the cutting tool along the width of the workpiece thus the cutting length was 8 mm. The hardness of the brass material workpiece was measured by Vickers testing on a Buehler Hardness Tester, which was 156.6 HV. A Kistler 9256C2 dynamometer was used to measure the cutting force components in the X, Y and Z directions. All the cutting experiments were full immersion slot milling, with a depth of cut 0.5 mm, a broad range of feedrate setting (0.5 to 3 μm/tooth), and a series of spindle speed varying from 10,000 rpm to 16,000 rpm. A photograph of the experimental setup is shown in Figure 9.

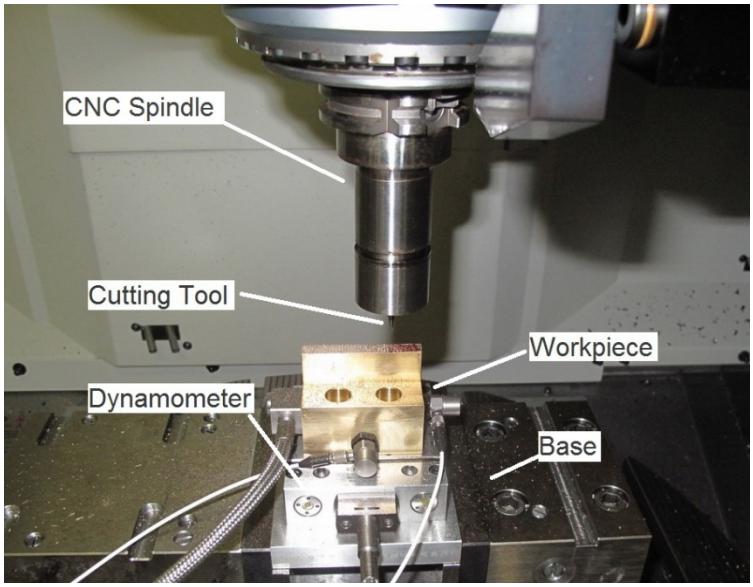

Figure 9 Experimental Setup

A group of comparisons of the cutting force components in *x* and *y* directions between the experiments and simulation by using the developed force model are given in Figures 10-14. In the simulation, the cutter runout value is practically set as the feed per tooth or close to it as the cutting force generated by a second tooth pass cannot be completely detected in the cutting tests on brass. The prediction and the experiment set in same conditions (feedrate, depth of cut, full immersion) are used to give following comparisons. It can be seen that the simulated cutting force waveform agrees well with the experimental results in terms of the force pulsation and general pattern, though there appears a slight underestimation of the peak force values in the y direction.

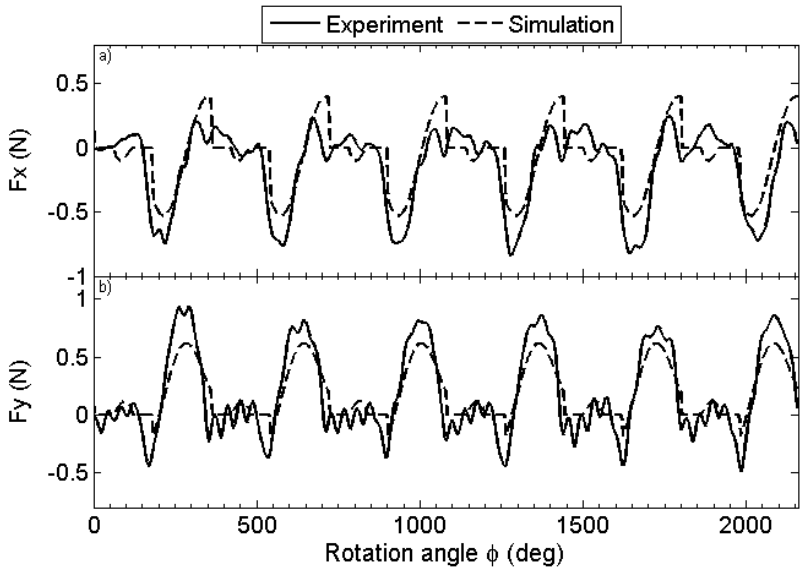

Figure 10 Comparison of cutting forces at Ω = 10,000 rpm, f_t= 3 μm/tooth, a = 50 μm.

Material: brass.

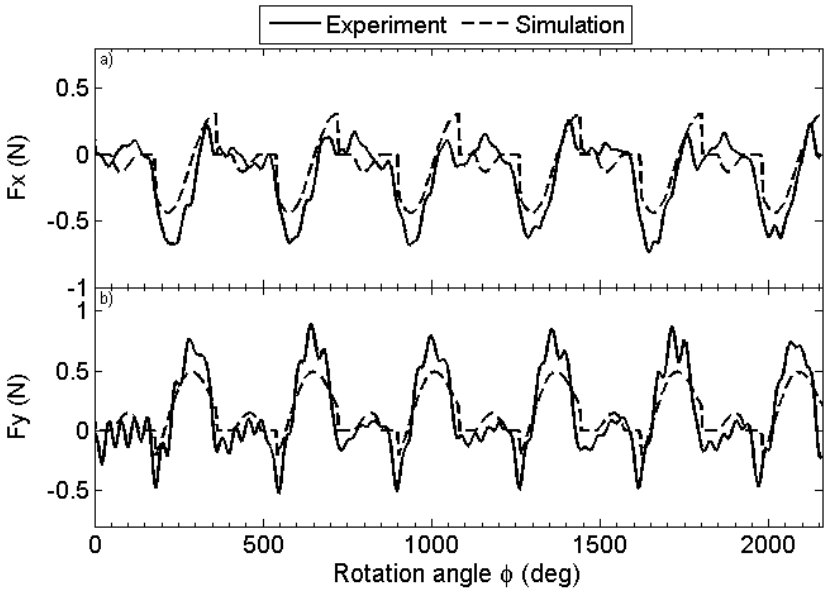

Figure 11 Comparison of cutting forces at Ω = 10,000 rpm, f_t= 2 μm/tooth, a = 50 μm.

Material: brass.

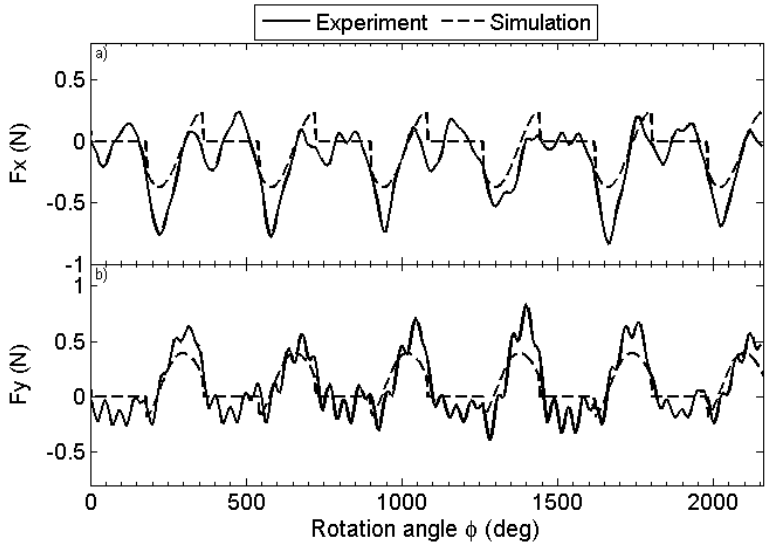

Figure 12 Comparison of cutting forces at Ω = 12,000 rpm, f_t= 1 μm/tooth, a = 50 μm. Material: brass.

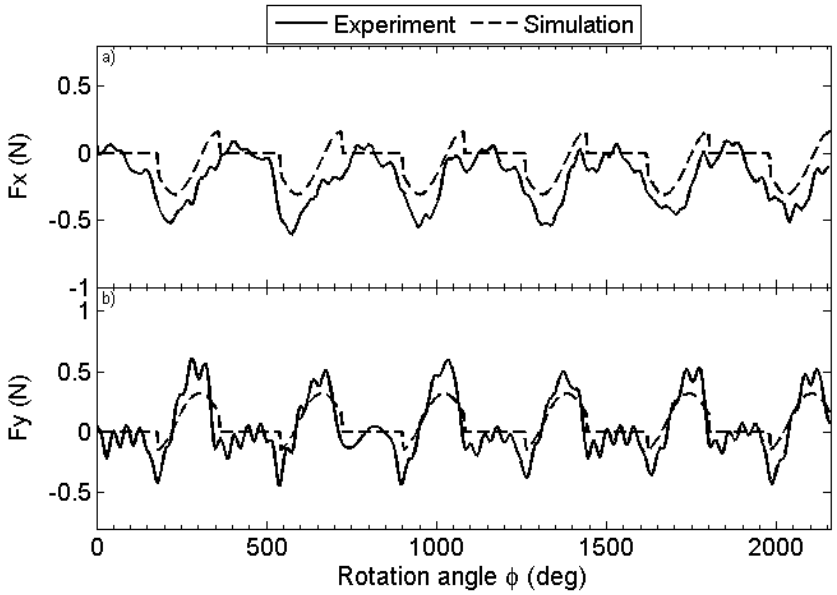

Figure 13 Comparison of cutting forces at Ω = 12,000 rpm, f_t= 0.5 μm/tooth, a = 50 μm. Material: brass.

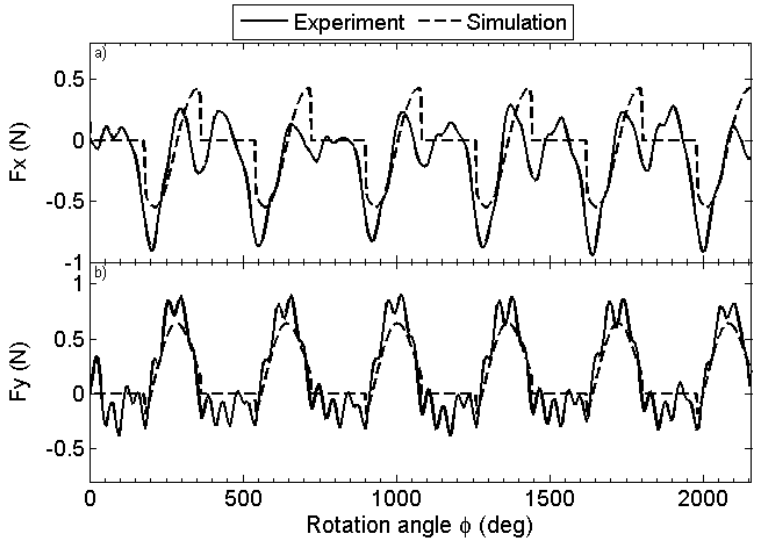

Figure 14 Comparison of cutting forces at Ω = 12,000 rpm, f_t= 3 μm/tooth, a = 50 μm. Material: brass.

The comparisons of average peak forces between the measurement and the prediction are presented in Figures 15 and 16. As the measured forces are of oscillating nature due to the tool-workpiece vibrations during the cutting operation, a low pass filter is applied to the measured force signals. The peak force is measured in each tool revolution considering the average force per tooth passing cycle. By fixing a starting point of the force profile for one revolution of the cutter, the set of data samples for each tooth passing cycle can be identified since the sampling frequency of data acquisition is known. These sets of data are averaged over a large group of cycles in the cutting process, then the results of cutting force components in *x* and *y* directions are finally presented.

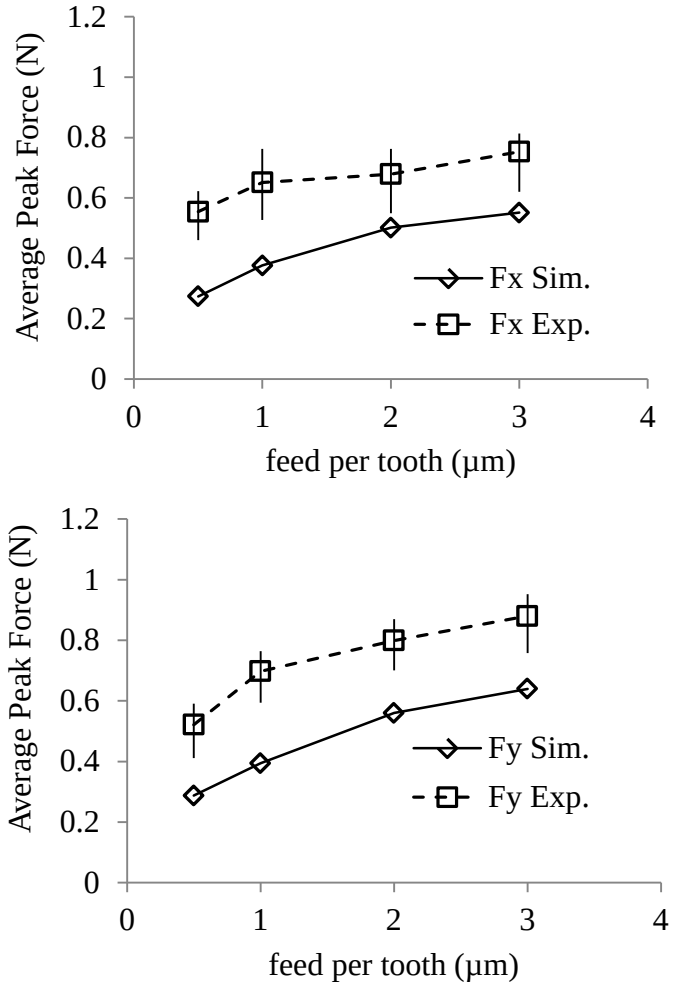

Figure 15 Comparison of the predicted and experimental peak amplitude of cutting force components for the two-flute cutter at different feed per tooth (cutting conditions: 10000 rpm; 0.05 mm depth of cut).

It can be seen that there exists a good agreement between the simulation and the experiments in terms of the general trend for the variation of the peak force against the cutting parameters. With the increase of the feed per tooth, the averaged peak force components in both x and y directions also increase, but with a slightly decreasing rate. As to the increment of the axial depth of cut, the peak force components also increase, in a slightly increasing rate. The simulation results

demonstrated the same trends on the influence of the feed and depth of cut. It should be noted that the magnitude of peak force is not well predicted with some underestimation. This might be due to the significant dynamic effects in the cutting experiment, which caused increased peak force values because of the tool-workpiece vibration. The current force model does not take into account the influence of the process dynamics, and it should be a topic for further development.

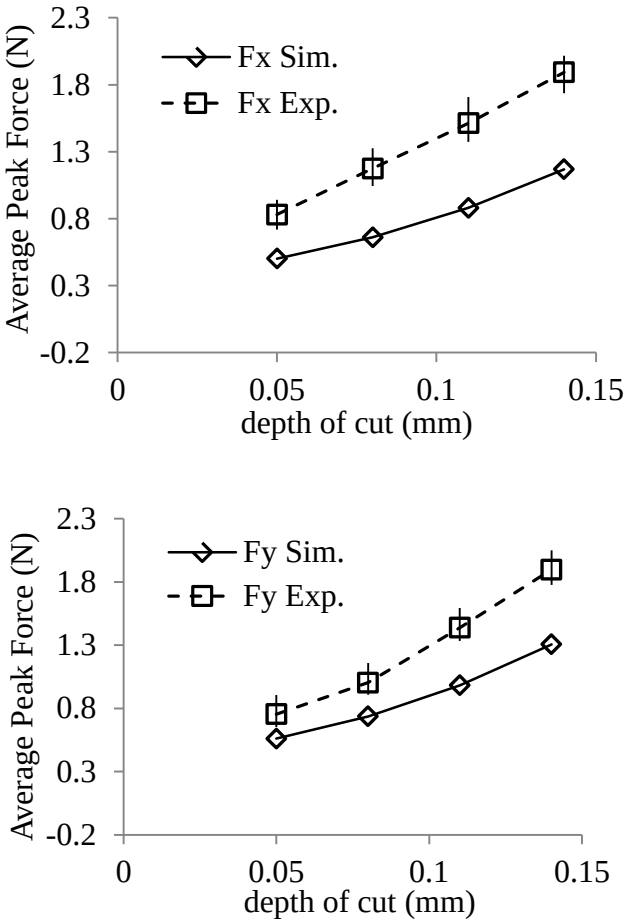

Figure 16 Comparison of the predicted and experimental peak amplitude of cutting force components for the two-flute cutter at different depth of cut (cutting conditions: 12000 rpm; 2 μm feed per tooth)

4. Conclusions

This paper introduced the development of a hybrid two-dimensional cutting force model in micromilling of brass based on results from numerical investigation of micro orthogonal cutting. FEA-based numerical simulation is employed to obtain the coefficients so that the characteristics of micro machining can be taken into account. The flow stress of workpiece material is modelled by using the Johnson-Cook constitutive material law. The cutting force coefficients are extracted from the FEA simulation and are modelled as a function of instantaneous uncut chip thickness, which is independent of cutting speed but influenced by tool edge radius. A new approach is developed to rectify the issue of sharp increase of the force coefficients under very small uncut chip thickness. It introduces a critical uncut chip thickness value and adjusts the coefficients by using a tangent slope for uncut chip thickness smaller than the critical value. A generalized analytical force model based on numerical findings is developed to predict the micro milling force by considering the tool trajectory and tool runout.

The simulation results of micro milling forces are compared against experimental measurement, where an agreement of force trends is shown along with the increasing feedrate and depth of cut. The proposed model closely predicts the cutting force waveforms along with the cutter rotation, while predicting the trend of peak force along with increasing feedrate and depth of cut meets the agreement with measured result. Further investigation on dynamic effect may be conducted to improve the accuracy of the model.

A limitation in this modelling approach is that the cutting force coefficients are derived from 2D FE simulation, the cutting action of an individual tooth segment is approximated as orthogonal cutting, and hence only the cutting force components in the *xy* plane normal to micro mill cutter axis can be determined. To account for the actual oblique cutting action of a cutting tooth segment, further research by using 3D FE simulation should be conducted. Further, the sensitivity of the Johnson-Cook model to some features in micromachining should also be assessed.

Acknowledgements

The authors would like to thank UNSW Australia for the support to this study.

References

[1] Li H, Jing X, Wang J. Detection and analysis of chatter occurrence in micro-milling process. Proc Inst Mech Eng Part B J Eng Manuf 2014;228:1359–71. doi:10.1177/0954405414522216.

[2] Jing X, Li H, Wang J, Tian Y. Modelling the cutting forces in micro-end-milling using a hybrid approach. Int J Adv Manuf Technol 2014;73:1647–56. doi:10.1007/s00170-014-5953-x.

[3] Liu X, DeVor RE, Kapoor SG, Ehmann KF. The Mechanics of Machining at the Microscale: Assessment of the Current State of the Science. J Manuf Sci Eng 2004;126:666. doi:10.1115/1.1813469.

[4] Yoon HS, Ehmann KF. Dynamics and stability of micro-cutting operations. Int

J Mech Sci 2016;115-116:81–92. doi:10.1016/j.ijmecsci.2016.06.009.

[5] Liu X, Jun MBG, DeVor RE, Kapoor SG. Cutting Mechanisms and Their Influence on Dynamic Forces, Vibrations and Stability in Micro-Endmilling. Manuf Eng Mater Handl Eng 2004;2004:583–92. doi:10.1115/IMECE2004-62416.

[6] Vogler MP, DeVor RE, Kapoor SG. On the Modeling and Analysis of Machining Performance in Micro-Endmilling, Part I: Surface Generation. J Manuf Sci Eng 2004;126:685–94. doi:10.1115/1.1813470.

[7] Vogler MP, DeVor RE, Kapoor SG. On the Modeling and Analysis of Machining Performance in Micro-Endmilling, Part II: Cutting Force Prediction. J Manuf Sci Eng 2004;126:695–705. doi:10.1115/1.1813470.

[8] Aramcharoen A, Mativenga PT. Size effect and tool geometry in micromilling of tool steel. Precis Eng 2009;33:402–7. doi:10.1016/j.precisioneng.2008.11.002.

[9] Yuan ZJ, Zhou M, Dong S. Effect of diamond tool sharpness on minimum cutting thickness and cutting surface integrity in ultraprecision machining. J Mater Process Technol 1996;62:327–30. doi:10.1016/S0924-0136(96)02429-6.

[10] Bao WY, Tansel IN. Modeling micro-end-milling operations. Part I: analytical cutting force model. Int J Mach Tools Manuf 2000;40:2155–73. doi:10.1016/S0890-6955(00)00054-7.

[11] Tlusty J, Macneil P. Dynamics of cutting forces in end milling. Ann CIRP 1975;24:21–5.

[12] Zaman MT, Kumar AS, Rahman M, Sreeram S. A three-dimensional analytical cutting force model for micro end milling operation. Int J Mach Tools Manuf 2006;46:353–66. doi:10.1016/j.ijmachtools.2005.05.021.

[13] Kang IS, Kim JS, Kim JH, Kang MC, Seo YW. A mechanistic model of cutting force in the micro end milling process. J Mater Process Technol 2007;187-188:250–5. doi:10.1016/j.jmatprotec.2006.11.155.

[14] Park SS, Malekian M. Mechanistic modeling and accurate measurement of micro end milling forces. CIRP Ann - Manuf Technol 2009;58:49–52. doi:10.1016/j.cirp.2009.03.060.

[15] Srinivasa Y V., Shunmugam MS. Mechanistic model for prediction of cutting forces in micro end-milling and experimental comparison. Int J Mach Tools Manuf 2013;67:18–27. doi:10.1016/j.ijmachtools.2012.12.004.

[16] Liu K, Melkote SN. Finite element analysis of the influence of tool edge radius on size effect in orthogonal micro-cutting process. Int J Mech Sci 2007;49:650–60. doi:10.1016/j.ijmecsci.2006.09.012.

[17] Jin X, Altintas Y. Prediction of micro-milling forces with finite element method. J Mater Process Technol 2012;212:542–52. doi:10.1016/j.jmatprotec.2011.05.020.

[18] Liang Y-C, Bai Q-S, Chen J-X. Modelling and Simulation of Micro Cutting. In: Cheng K, Huo D, editors. Micro-Cutting Fundam. Appl. 1st ed., John Wiley & Sons, Ltd.; 2013, p. 115–51.

[19] Gau J-T, Principe C, Yu M. Springback behavior of brass in micro sheet forming. J Mater Process Technol 2007;191:7–10.

doi:10.1016/j.jmatprotec.2007.03.035.

[20] Gordon R. Johnson, Cook WH. A constitutive model and data for metals subjected to large strains, high strain rates and high temperatures.pdf. Int Symp Ballist 1983:541–7.

[21] Lauro CH, Brandão LC, Filho SLMR, Valente RAF, Davim JP. Finite Element Method in Machining Processes: A Review. In: Davim JP, editor. Mod. Manuf. Eng., Springer International Publishing; 2015, p. 65–97. doi:10.1007/978-3-319-20152-8_3.

[22] Wang J, Gong Y, Abba G, Antoine JF, Shi J. Chip formation analysis in micromilling operation. Int J Adv Manuf Technol 2009;45:430–47. doi:10.1007/s00170-009-1989-8.

[23] Ucun İ, Aslantas K, Bedir F. Finite element modeling of micro-milling: Numerical simulation and experimental validation. Mach Sci Technol 2016;20:148–72. doi:10.1080/10910344.2016.1147650.

[24] Li HZ, Liu K, Li XP. A new method for determining the undeformed chip thickness in milling. J Mater Process Technol 2001;113:378–84. doi:10.1016/S0924-0136(01)00586-6.

[25] Li HZ, Zhang WB, Li XP. Modelling of cutting forces in helical end milling using a predictive machining theory. Int J Mech Sci 2001;43:1711–30. doi:10.1016/S0020-7403(01)00020-0.